

Douglas R. Allen, Stephen D. Eckermann, Lawrence Coy, and John P. McCormack
Naval Research Laboratory
Washington, DC 20375

Timothy F. Hogan and Young-Joon Kim
Naval Research Laboratory
Monterey, CA 93943

ABSTRACT

A new high-altitude version of the Navy Operational Global Atmospheric Prediction System (NOGAPS) is described and used to hindcast the unusual 2002 Antarctic stratospheric major warming. The new version, called NOGAPS-Advanced Level Physics with High Altitude (NOGAPS-ALPHA or NOGAPS- α) includes modifications to multiple components of the operational version, including the radiation scheme, gravity wave drag, vertical coordinate, and meteorological initialization. It also has a raised model top from 1.0 to 0.005 hPa and radiatively active prognostic ozone with parameterized photochemistry. A detailed comparison of the major warming period (September 2002) is done with operational NOGAPS (NOGAPS-op), operational ECMWF, and NOGAPS- α stratospheric forecasts. We examine the synoptic evolution of the middle stratospheric polar vortex as well as wave propagation diagnostics. The NOGAPS-op forecasts showed weaker wave activity compared to the analysis, which resulted in poorer predictions of the split stratospheric vortex. The situation improved in NOGAPS- α forecasts initialized with NOGAPS operational analyses, with stronger wave amplitudes and better forecasting of the split vortex. More significant improvements were found when NOGAPS- α was initialized with the ECMWF analyses, prompting plans for a NOGAPS re-analysis of this period.

1. INTRODUCTION

This paper examines stratospheric forecasts from a new high-altitude version of the Navy Operational Global Atmospheric Prediction System (NOGAPS). NOGAPS is the Department of Defense's high-resolution global numerical weather prediction (NWP) system. Its development and operation is a joint activity of the Naval Research Lab (NRL) and the Navy's Fleet Numerical Meteorology and Oceanography Center (FNMOC). Hogan and Rosmond (1991) and Hogan et al. (1991) provide thorough descriptions of the NOGAPS forecast model.

In October 2000, NRL initiated a research project to extend NOGAPS from its current 1 hPa upper boundary to include a fully-resolved prognostic middle atmosphere. This project is ongoing: the goal is to progressively transition aspects of this new NOGAPS with Advanced-Level Physics and High Altitude (NOGAPS-ALPHA or NOGAPS- α) to FNMOC as a next-generation high-altitude operational NOGAPS that improves NWP at all levels (e.g., improved operational assimilation of satellite radiances).

A new family of physics packages were needed to adequately simulate the new upper altitudes of the prognostic NOGAPS atmosphere (for details see Eckermann et al.,

2004). These include new radiation and gravity wave drag schemes, new meteorological initialization, and new prognostic capabilities for ozone and other tracers. NOGAPS- α also replaces the current sigma coordinate with hybrid vertical levels that transition from terrain-following near the surface to pure pressure levels at ~ 85 hPa. Our current T239L54 model uses a new hybrid formulation that, as shown in Figure 1, produces uniformly smooth transitions to constant pressure height thicknesses in the stratosphere over arbitrary topography, and adopts constant pressure height thicknesses throughout the rest of the middle atmosphere. This uniform vertical resolution offers better resolved middle atmosphere dynamics.

For initialization of NOGAPS- α , we use the “cold start” procedure in which analyzed winds, moisture, and geopotential heights on pressure surfaces are interpolated to the model levels (temperature is thereby calculated from the heights using hydrostatic balance). Operationally assimilated meteorological fields at FNMOC only extend to 10 hPa at present, though an experimental “STRATOI” product is also issued based mostly on TIROS Operational Vertical Sounder (TOVS) radiances, which yields additional initialization for winds and temperatures up to 0.4 hPa. Unfortunately, the STRATOI fields were not archived during this period, so we have opted to use ECMWF analyzed winds and layer thicknesses for the region from 10-1 hPa. Given our current upper boundary of 0.005 hPa, we have developed a generalized upper-level initialization scheme within NOGAPS- α that extrapolates topmost initialization wind, temperature and geopotential fields by progressively relaxing them with increasing altitude to climatological values from the CIRA 1986 (Fleming et al., 1990) or UARS (Swinbank and Ortland, 2003) reference atmospheres.

The UARS initialization is used in all the NOGAPS- α forecasts in this paper.

2. STRATOSPHERIC FORECASTING WITH NOGAPS- α

Here we compare stratospheric forecasts from the operational NOGAPS model (denoted by NOGAPS-op), NOGAPS- α , and ECMWF for the unusual 2002 Southern Hemisphere (SH) stratospheric major warming. This event provides an opportunity to examine the dynamics of the SH stratosphere during conditions unlike anything observed previously. The highly active 2002 winter was capped in late September by rapid enhancement of zonal waves 1, 2, and 3 in the geopotential height in the middle stratosphere (10 hPa) that accompanied the splitting of the winter polar vortex (and therefore the Antarctic ozone hole) and record warming of the vortex in late September (Baldwin et al., 2003; Allen et al., 2003; Sinnhuber et al., 2004; Weber et al., 2004). This was due to unusually strong tropospheric wave forcing; observations showed that in 2002 the 100 hPa eddy heat flux preceding the warming was significantly larger than that seen in any previous year (Allen et al., 2003; Sinnhuber et al., 2003; Weber et al., 2003). A remarkable aspect of this event is that it was predicted by operational weather forecasts up to about a week in advance (Simmons et al., 2004). The ECMWF meteorological forecasts were also used with an offline ozone assimilation system to drive ozone forecasts, which predicted the splitting Antarctic ozone hole (Eskes et al., 2004).

We first examine synoptic plots of the 10 hPa geopotential height for forecasts initialized 20 September 2002 (12Z). Figure 2 shows the ECMWF analyses (top row) compared with 5-day forecasts. The analyses show the vortex initially slightly

elongated and centered off the pole. A weak anticyclonic circulation exists south and west of Australia. From 21-22 September, the vortex is pushed off the pole as the anticyclone strengthens, causing a strong zonal wave 1 pattern. The vortex further elongates and by 23 September forms two distinct cyclonic cells. These separate further until 25 September, when the vortex splits into two pieces (here we identify a “split” vortex as that in which there are no closed contours surrounding both vortex cells). The splitting of the vortex at 10 hPa has never been observed in the SH during this time of year. The vortex usually remains intact until the final warming around November/December.

The ECMWF forecast for this event closely matches the analysis. The growing anticyclone distorts the vortex, which splits on 25 September. The NOGAPS-op 5-day forecast similarly shows a strengthening anticyclone south of Australia and a vortex that forms two cells. However, the vortex doesn’t completely split by 25 September, indicating smaller wave amplitudes, particularly zonal components 2 and 3 (more below).

Two NOGAPS- α forecasts were run for comparison. The first was initialized as described in Section 1, using NOGAPS analyses from 1000-10 hPa and ECMWF analyses from 10-1 hPa, while the second was initialized using ECMWF analyses from 1000-1 hPa. We will distinguish these runs as NOGAPS- α (nog) and NOGAPS- α (ecm). The NOGAPS- α (nog) forecast is very similar to NOGAPS-op, although the two cells on 25 September are slightly nearer separation on 25 September in NOGAPS- α (nog). The NOGAPS- α (ecm) forecast is initially somewhat noisy. This is due to slight mismatch in the lower boundary fields when using the ECMWF pressure level data. This small-scale noise rapidly damps out during the model run. The resulting 5-day

forecast shows a vortex split, seemingly in better agreement with the analyses.

To quantify differences between these 5-day forecasts, we next examine the geopotential height zonal wave amplitudes at 10 hPa. Figure 3 shows the wave 1, 2, and 3 amplitudes for the SH on 25 September (5-day forecast). The analyses show the wave 1 amplitude to peak at around 1100 m near 65 S. While the ECMWF forecast captures this wave quite well, the NOGAPS-op wave 1 is much too strong. Similarly, the NOGAPS- α (nog) wave 1 is too strong, but is in closer agreement with the analyses than NOGAPS-op. The NOGAPS- α (ecm) wave 1 agrees much better with ECMWF, suggesting that the results are strongly dependent on the initial conditions. The analyses show wave 2 and wave 3 amplitudes peaking near 60 S with values of around 860 and 670 m. Here again, the ECMWF forecast captures the waves well, but in this case the NOGAPS-op underestimates the wave amplitudes, especially wave 2. NOGAPS- α (nog) also underestimates the W2 and W3 amplitudes, although not as much as NOGAPS-op, while NOGAPS- α (ecm) somewhat overestimates the W2 and W3 amplitudes at this level.

That NOGAPS- α (nog) does better than NOGAPS-op at 10 hPa is not a surprise, given the much higher vertical resolution (see Fig. 1). Analysis of wave amplitudes lower down, at 30 and 50 hPa (not shown) and 100 hPa (Figure 4), indicate that NOGAPS-op consistently overestimates the amplitude of wave 1 and underestimates the amplitudes of waves 2 and 3. NOGAPS- α (nog) agrees better with the analyses at 100 hPa than NOGAPS-op in nearly all cases, while NOGAPS- α (ecm) often shows some additional improvement over NOGAPS- α (nog). Manney et al. (2004) performed mechanistic model studies of this event using a GCM with a lower boundary at 100 hPa. They showed that the stratospheric major warming was well

simulated when the lower boundary was forced by observed (analyzed) 100 hPa geopotential height fields. They found that the model was particularly sensitive to the amplitudes of the three largest waves (zonal waves 1, 2, and 3) at 100 hPa. Even a small reduction (25 %) in the zonal wave 2 amplitude resulted in a vortex at 10 hPa that didn't completely split. It is likely that the larger wave 2 and 3 forcing in NOGAPS- α at 100 hPa is contributing to the better forecasts in the middle stratosphere.

An additional measure of wave propagation is the eddy heat flux, which is proportional to the upward group velocity. Allen et al. (2003) showed that the magnitude of this quantity (averaged from 45-75 S) in late September 2002 was more than twice that observed in previous years (1979-2001). This unusually large heat flux is clearly linked to the large stratospheric waves that split the vortex (e.g., Newman and Nash, 2004). In Figure 5 we show the 5-day forecasted heat flux at 10, 30, and 50 hPa. It is interesting that all models underestimate the analyzed heat flux at all three levels. However, NOGAPS-op is consistently much lower than ECMWF. NOGAPS- α (nog) tends to show larger heat flux than NOGAPS-op, particularly at 10 hPa, while NOGAPS- α (ecm) shows even larger values, in better agreement with ECMWF.

Although the heat flux at 10 hPa peaks on 25 September, at lower levels the heat flux peaks earlier, an indication of upward propagating wave energy. For example, at 100 hPa the heat flux peaks on 22 September, while at 200 hPa it peaks on 21 September. Figure 6 shows heat flux at initialization and first two days of the forecasts at these two levels. At initialization, the 200 hPa heat flux shows some rather large differences between NOGAPS and ECMWF. The NOGAPS-op and NOGAPS- α (nog) runs (both initialized

with NOGAPS operational analyses) show significantly lower heat flux than the ECMWF analyses. This discrepancy is not unusual. Newman and Nash (2000) compared eddy heat fluxes calculated from five different meteorological analyses and showed that they differ on average by around 15%. NOGAPS- α (ecm) shows in between values. That NOGAPS- α (ecm) does not agree with the ECMWF analyses at initialization is likely due to the balancing that is performed during the "cold start" initialization procedure described in Section 1. At 100 hPa, however, the initial heat fluxes are similar in magnitude, although the ECMWF flux shows a broader peak. Over the next two days, it is clear that the 100 hPa heat flux grows too slowly in the NOGAPS-op and NOGAPS- α (nog) runs. This is likely due to the reduced upward wave forcing seen in the 200 hPa fields.

To examine the overall forecast skill for these runs we calculated the RMS temperature difference with respect to the ECMWF analysis, covering the latitude range 30-90 S (calculated using $\cos(\text{latitude})$ weighting). The results at six pressure levels are shown in Figure 7. In all cases, the ECMWF forecasts have the best skill, with 5-day errors of between 1.5 and 3 K, varying with pressure. The NOGAPS-op forecasts show significantly larger errors, peaking between 4 and 10 K after 5-days. Using NOGAPS- α (nog) we find a large improvement at 10 hPa, although much of this is due to improved initial conditions. Recall that since NOGAPS analyses above 10 hPa were not archived for this period, we use ECMWF height information above 10 hPa for the NOGAPS- α (nog) initialization. Since the temperatures are calculated from the heights, some of the ECMWF information "leaks" into the 10 hPa temperatures. At 30 hPa and below, the NOGAPS-op and NOGAPS- α (nog) errors are similar out to 5-days, while NOGAPS- α

(ecm) shows consistently better agreement with ECMWF, as expected due to closer initial conditions.

We now examine forecasts for different initial dates. Figure 8 shows the 10 hPa geopotential height fields evaluated on 25 September for runs initialized on 20-23 September (2- to 5-day forecasts). Recall from Figure 2 that the ECMWF analysis shows a clean vortex split on 25 September (i.e., no closed contours). The NOGAPS operational 10 hPa analysis shows a similar vortex split on this date. Here the NOGAPS-op 2-day forecast clearly shows a split vortex, while the 3-5 day forecasts still have a closed contour around the two vortex cells. The NOGAPS- α (nog) forecasts show a split vortex out to 4-days, a 2-day improvement over NOGAPS-op. The NOGAPS- α (ecm) forecasts show a split vortex out to 5-days, as do the ECMWF operational forecasts (not shown). Actually, ECMWF data show a split vortex on 25 September for forecasts out to 7 days (Simmons et al., 2004).

The better resolution of the vortex splitting in NOGAPS- α compared with NOGAPS-op suggests improved wave growth and propagation in these forecasts. Figure 9 shows the amplitude of wave 2 at 60 S for 10, 50, and 100 hPa for forecasts initialized on 18, 19, 20, and 21 September. It is clear that the NOGAPS-op wave 2 amplitude underestimates the analyzed values at all levels and for all runs. The NOGAPS- α (nog) forecasts tend to show slightly larger wave amplitudes, suggesting that the higher vertical resolution in the lower stratosphere is helping to forecast the growth and propagation of the large-scale waves. The NOGAPS- α (ecm) forecasts tend to agree much better with the analyses and with the ECMWF forecasts, consistent with previous results.

As discussed earlier, due to the upward propagation of the large-scale waves, the quality of the middle

stratospheric forecasts will be strongly dependent on how well the model is forecasting the lower stratospheric waves. Here we examine how well each model was able to predict the peak value of the wave 2 amplitude at 100 hPa, 60 S, along with the peak value of the heat flux at 100 hPa (averaged over 45-75 S). Figure 10 shows these quantities as a function of initialization day from 17-22 September. The magnitude of the maximum analyzed heat flux peaked at 101 K m/s (indicated by a black line). The NOGAPS-op forecasts consistently underestimated this value, with lower peaks for earlier runs. NOGAPS- α (nog) shows a small but significant improvement over NOGAPS-OPS, with larger improvement for longer forecasts. NOGAPS- α (ecm) shows an additional improvement, particularly for initialization on 19-22 September. Similar results are found for the wave 2 amplitude. Figure 10 (right) shows that NOGAPS-op underestimates the analyzed maximum value of 511 m, NOGAPS- α (nog) shows a slight improvement, and NOGAPS- α (ecm) shows an additional significant improvement. For these diagnostics NOGAPS- α (ecm) actually slightly outperforms ECMWF for forecasts on 20-21 September, but ECMWF forecasts are better for the longer runs.

3. DISCUSSION

These results show that overall the NOGAPS operational forecasts for the 2002 SH major warming period underestimated the magnitude of the upward propagating large-scale planetary waves that split the middle stratospheric vortex. Runs with the new high-altitude NOGAPS- α , initialized with NOGAPS operational analyses, showed a small but consistent improvement over NOGAPS-op, likely due primarily to improvements in model vertical resolution in the stratosphere. More significant

improvements were observed when NOGAPS- α was run with ECMWF initial conditions. Larger wave 2 growth was observed from 100 to 10 hPa, and larger heat fluxes pointed to stronger upward propagation of energy. However, we note that all 5-day forecasts (initialized 20 September), including ECMWF, tended to underestimate the growth in heat flux at 10 hPa.

The sensitivity to initial conditions has prompted us to re-examine the NOGAPS operational analyses for this period. In particular, we are currently doing a re-analysis for September 2002 using the newly operational Navy Atmospheric Variational Data Assimilation System (NAVDAS), detailed in Daley and Barker (2001), which should improve on the then-operational multivariate optimal interpolation (MVOI) algorithm.

REFERENCES

- Allen, D. R., R. M. Bevilacqua, G. E. Nedoluha, C. E. Randall, and G. L. Manney, 2003: Unusual stratospheric transport and mixing during the 2002 Antarctic winter. *Geophys. Res. Lett.*, **30** (12), 1599, doi:10.1029/2003GL017117.
- Baldwin, M. P., T. Hirooka, A. O'Neill, and S. Yoden, 2002: Major stratospheric warming in the southern hemisphere in 2002: Dynamical aspects of the ozone hole split. *SPARC Newsletter*, **20**, 24-26.
- Daley, R., and E. Barker, 2001: NAVDAS: formulation and diagnostics, *Mon. Wea. Rev.*, **129**, 869-883.
- Eckermann, S. D., J. P. McCormack, L. Coy, D. Allen, T. Hogan, and Y.-J. Kim, 2004: NOGAPS-ALPHA: a prototype high-altitude global NWP model, *Preprint Vol. Symposium on the 50th Anniversary of Operational Numerical Weather Prediction*, American Meteorological Society, 14-17 June (this issue).
- Eskes, H., A. Segers, and P. van Velthoven, 2004: Ozone forecasts of the stratospheric polar vortex splitting event in September 2002, *J. Atmos. Sci.*, in press.
- Fleming, E.L., S. Chandra, J.J. Barnett, and M. Corney, 1990: Zonal mean temperature, pressure, zonal wind, and geopotential height as functions of latitude, COSPAR International Reference Atmosphere: 1986, Part II: Middle Atmosphere Models, *Adv. Space Res.*, **10** (12), 11-59.
- Hogan, T., and T. Rosmond, 1991: The description of the Navy Operational Global Atmospheric Prediction System's spectral forecast model, *Mon. Wea. Rev.* **119**, 1186-1815.
- Hogan, T. F., T. E. Rosmond, and R. Gelaro, 1991: The NOGAPS forecast model: a technical description, Naval Oceanographic and Atmospheric Research Laboratory Report No. 13, 219pp.
- Manney, G. L., and Coauthors, 2004: Simulations of dynamics and transport during the September 2002 Antarctic major warming, *J. Atmos. Sci.*, in press.
- Newman, P. A., and E. R. Nash, 2000: Quantifying the wave driving of the stratosphere, *J. Geophys. Res.*, **105** (10), 12,485-12,497.
- Newman, P. A., and E. R. Nash, 2004: The unusual southern hemisphere stratosphere winter of 2002, *J. Atmos. Sci.*, in press.
- Simmons, A., M. Hortal, G. Kelly, A. McNally, A. Untch, and S. Uppala, 2003: Analyses and forecasts of stratospheric

winter polar vortex break-up: September 2002 in the Southern Hemisphere and related events from ECMWF operations and ERA-40, ERA-40 Project Report Series no. 5, European Centre for Medium Range Weather Forecasts.

Sinnhuber, B.-M., M. Weber, A. Amankwah, and J. P. Burrows, 2003: Total ozone during the unusual Antarctic winter of 2002. *Geophys. Res. Lett.*, **30** (11), 1581, 10.1029/2003GL017086.

Swinbank, R., and D. A. Ortland, 2002: Compilation of wind data for the UARS reference atmosphere project, *Adv. Space Res.*, 2003.

Weber, M., S. Dhomse, F. Wittrock, A. Richter, B.-M. Sinnhuber, J. P. Burrows, 2003: Dynamical control of NH and SH winter/spring total ozone from GOME observations in 1995-2002. *Geophys. Res. Lett.*, **30** (11), 1583, 10.1029/2002GL016799.

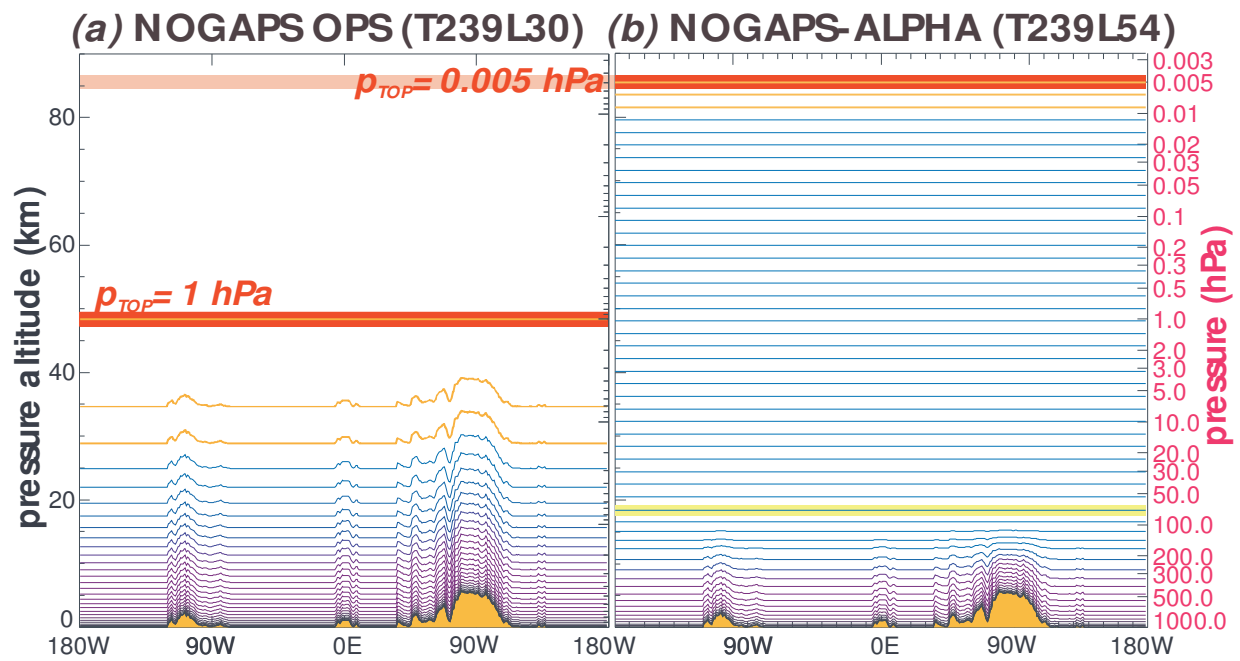


FIG. 1. Schematic of vertical levels around a latitude circle for (a) operational NOGAPS and (b) NOGAPS- α .

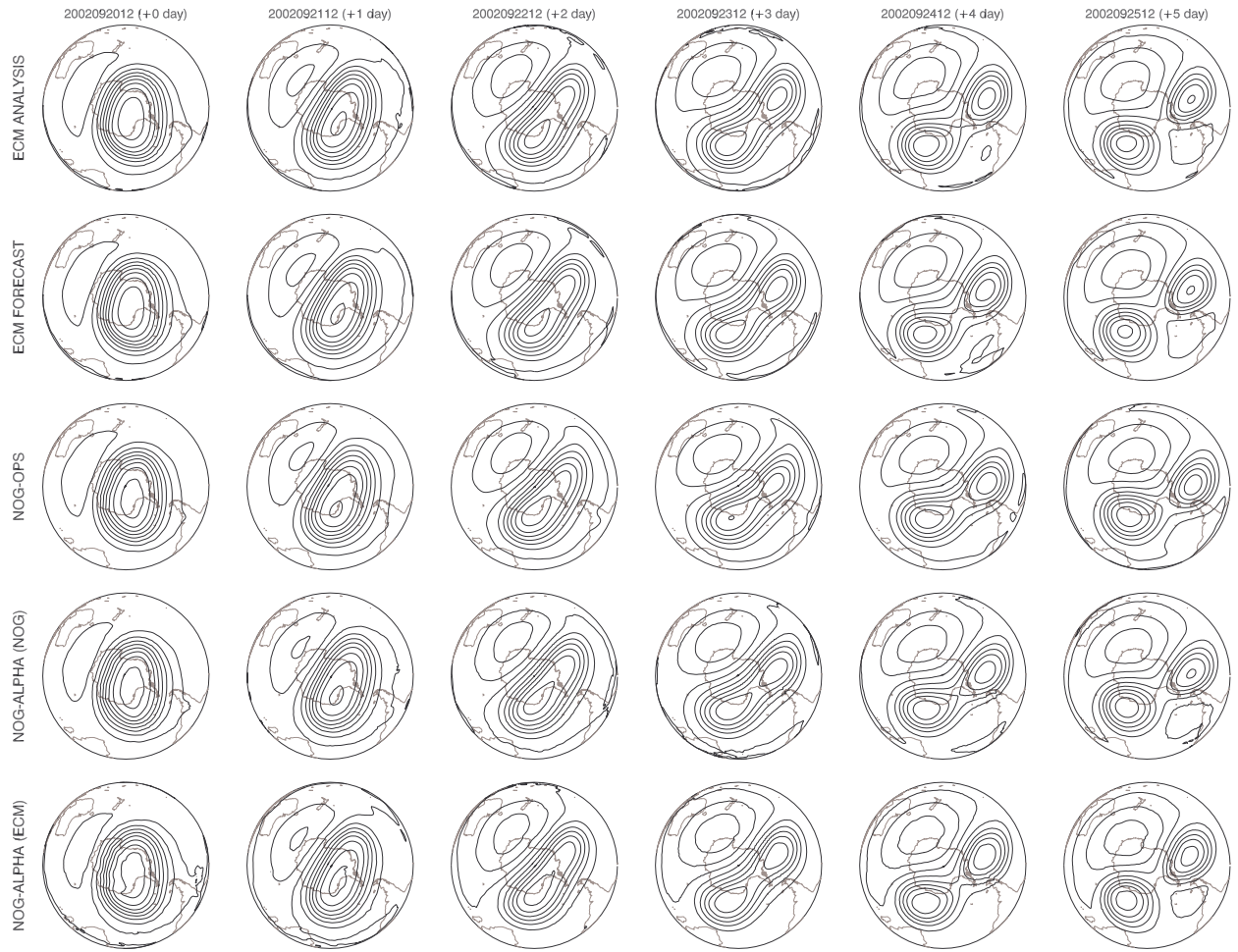


FIG. 2. Geopotential height at 10 hPa (~ 32 km) over the SH for 20-25 September 2002. The top row is the ECMWF analysis, while the next four rows are ECMWF forecast, NOGAPS operational forecast, and NOGAPS- α forecasts initialized with NOGAPS and ECMWF initial conditions. All forecasts were initialized at 12 Z on 20 September 2002. Contour interval is 400 m.

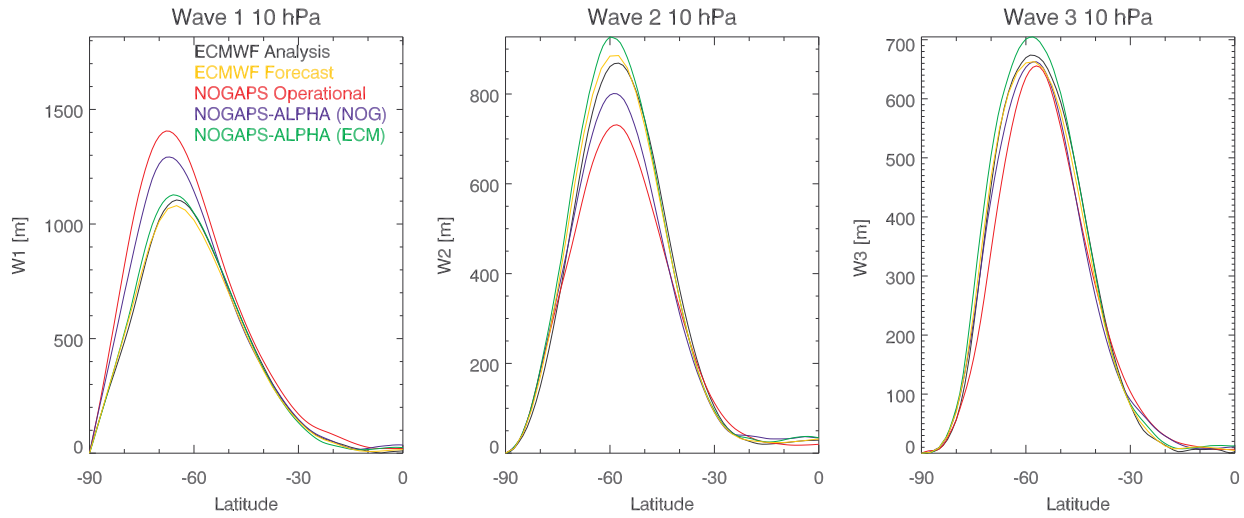


FIG. 3. Geopotential height zonal wave 1, 2, and 3 amplitudes at 10 hPa (~ 32 km) over the SH for 5-day forecasts initialized 20 September 2002. The colors determine the particular run, as indicated in the first plot.

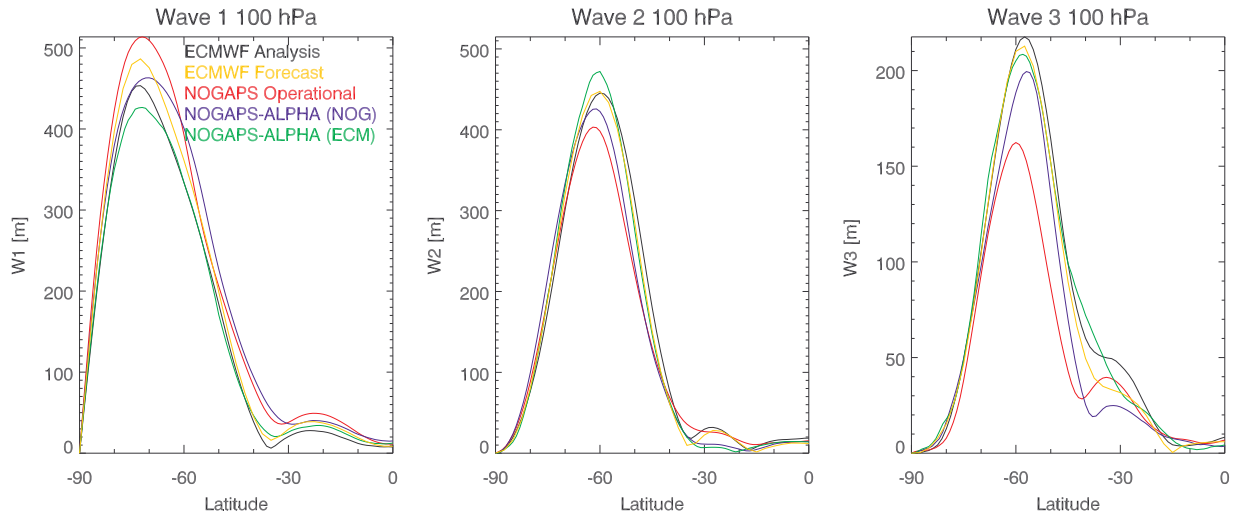


FIG. 4. Geopotential height wave 1, 2, and 3 amplitudes at 100 hPa over the SH for 5-day forecast initialized 20 September 2002. The colors determine the particular run, as indicated in the first plot.

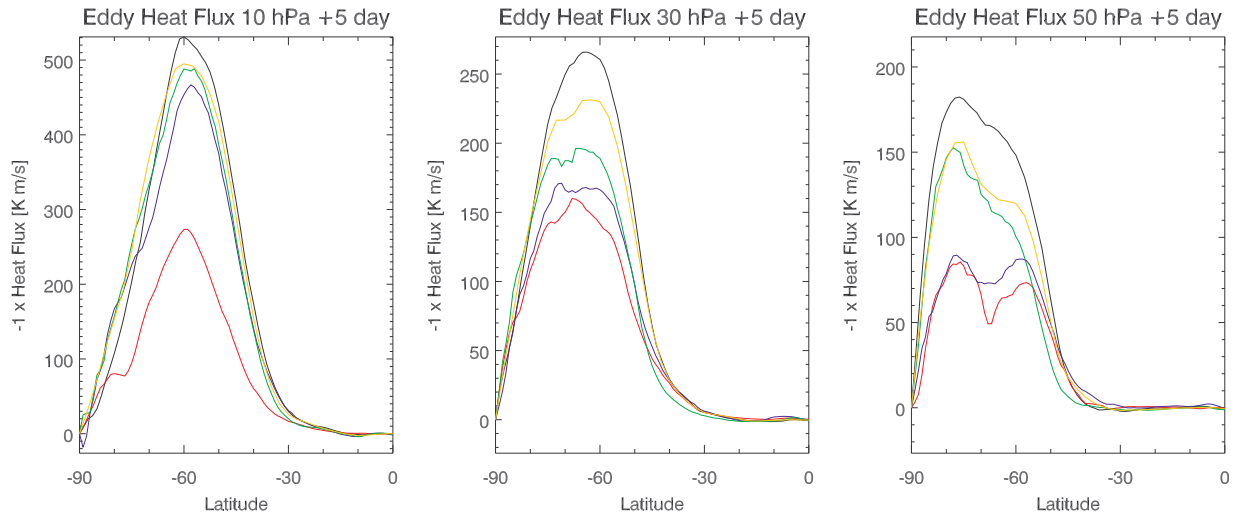


FIG. 5. Eddy heat flux (multiplied by -1 to make poleward flux positive) at 10, 30, and 50 hPa over the SH for 5-day forecast initialized 20 September 2002. The colors for each forecast are as indicated in Figure 3.

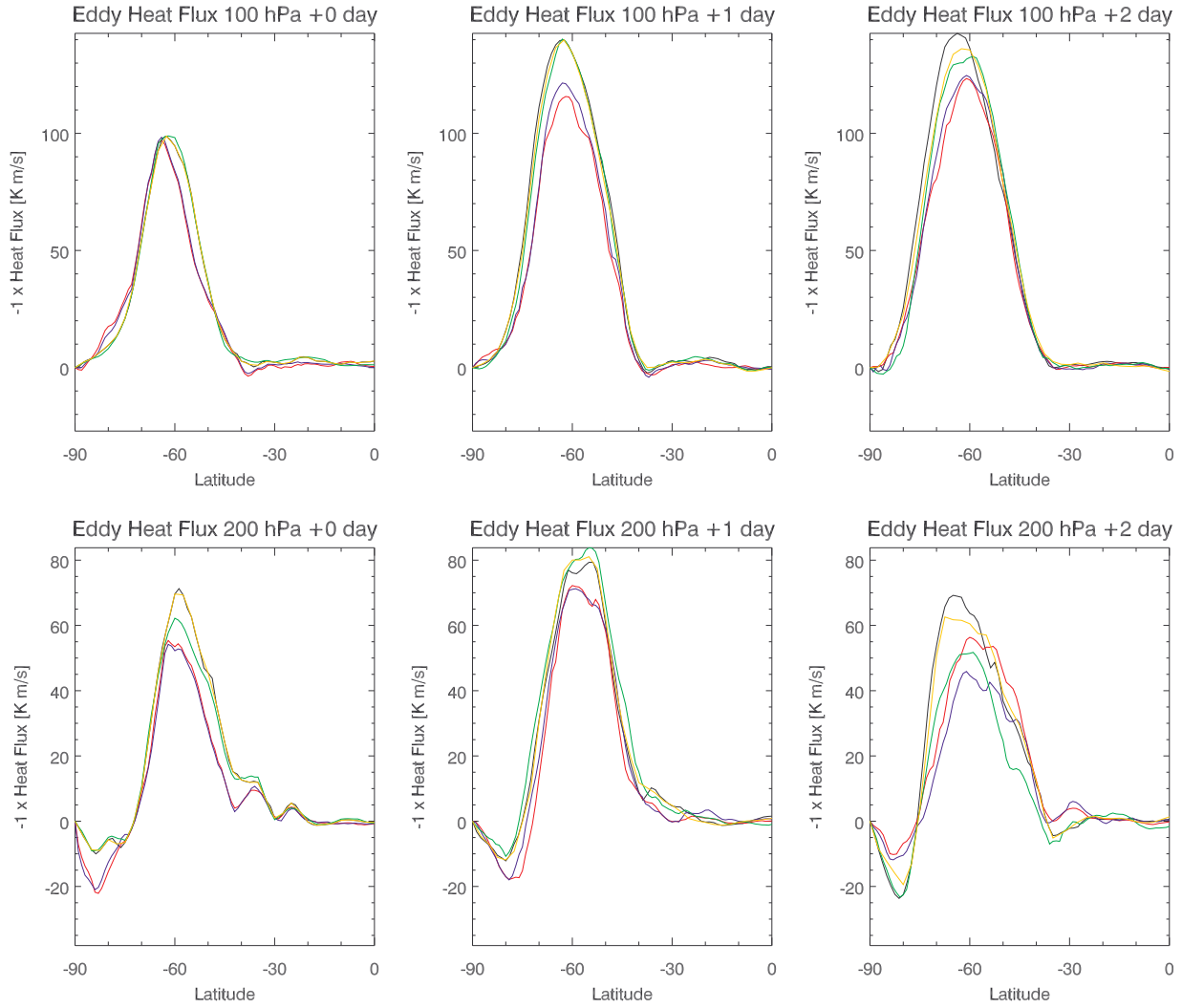


FIG. 6. Eddy heat flux (multiplied by -1 to make poleward flux positive) at 100 and 200 hPa over the SH for initialization, and 1- and 2-day forecasts initialized 20 September 2002. The colors for each forecast are as indicated in Figure 3.

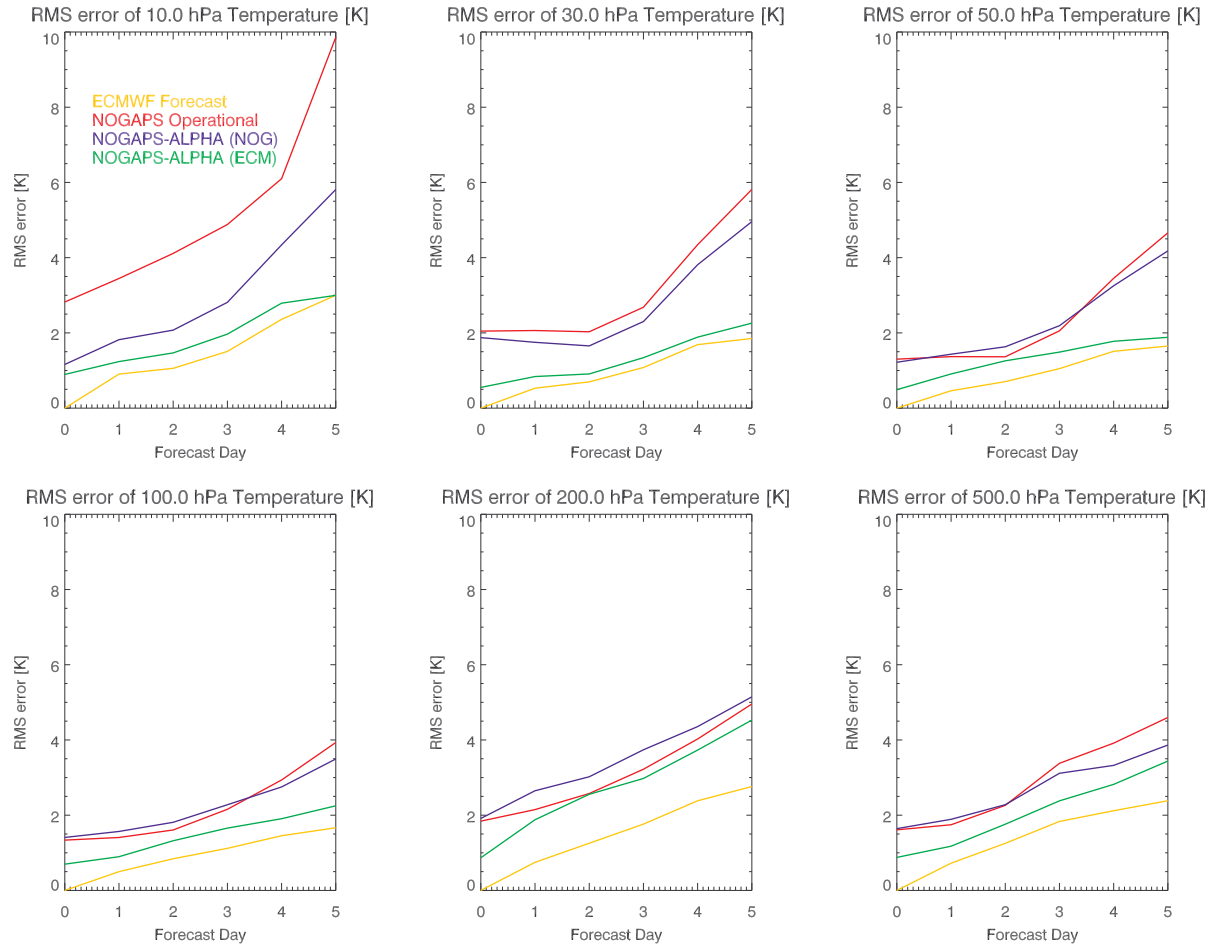


FIG. 7. Root-mean-square temperature error for forecasts initialized 20 September 2002 for the latitude range 30-90 S. The error is calculated with respect to the ECMWF analyses. The colors for each forecast are as indicated in the first panel. The calculation is done separately at 10, 30, 50, 100, 200, and 500 hPa.

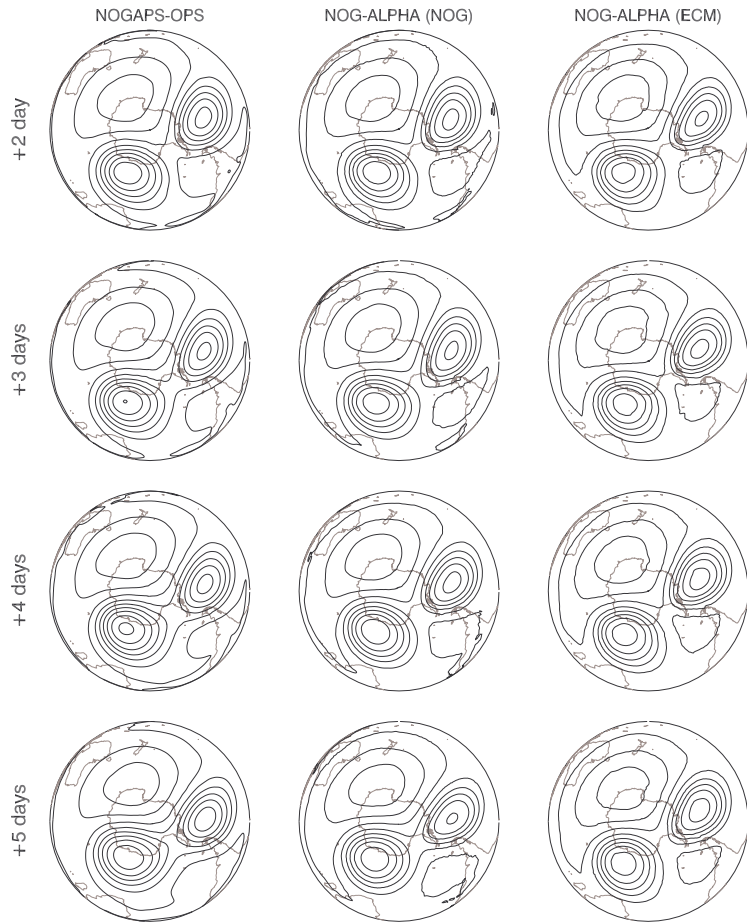


FIG. 8. Geopotential height at 10 hPa (~ 32 km) over the SH for forecasts evaluated at 25 September 2002. The left column is the NOGAPS operational analysis, the middle column is NOGAPS- α (nog), and the right column is NOGAPS- α (ecm). The length of forecast is provided on the left hand side. Contour interval is 400 m.

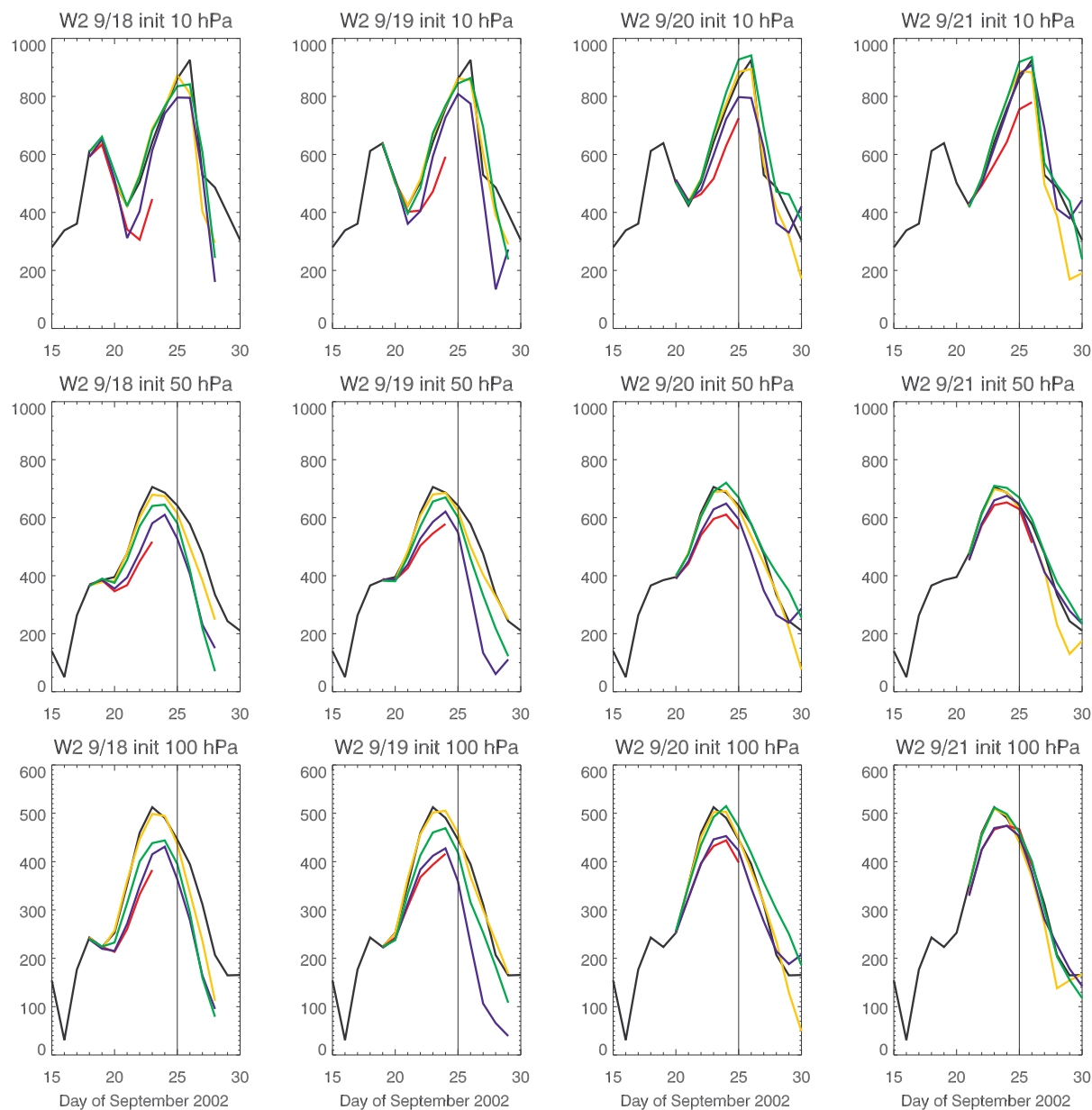


FIG. 9. Geopotential height zonal wave 2 amplitude at 10, 50, and 100 hPa and 60 S for forecasts initialized 18, 19, 20, 21 September 2002. The colors for each forecast are as indicated in Figure 3.

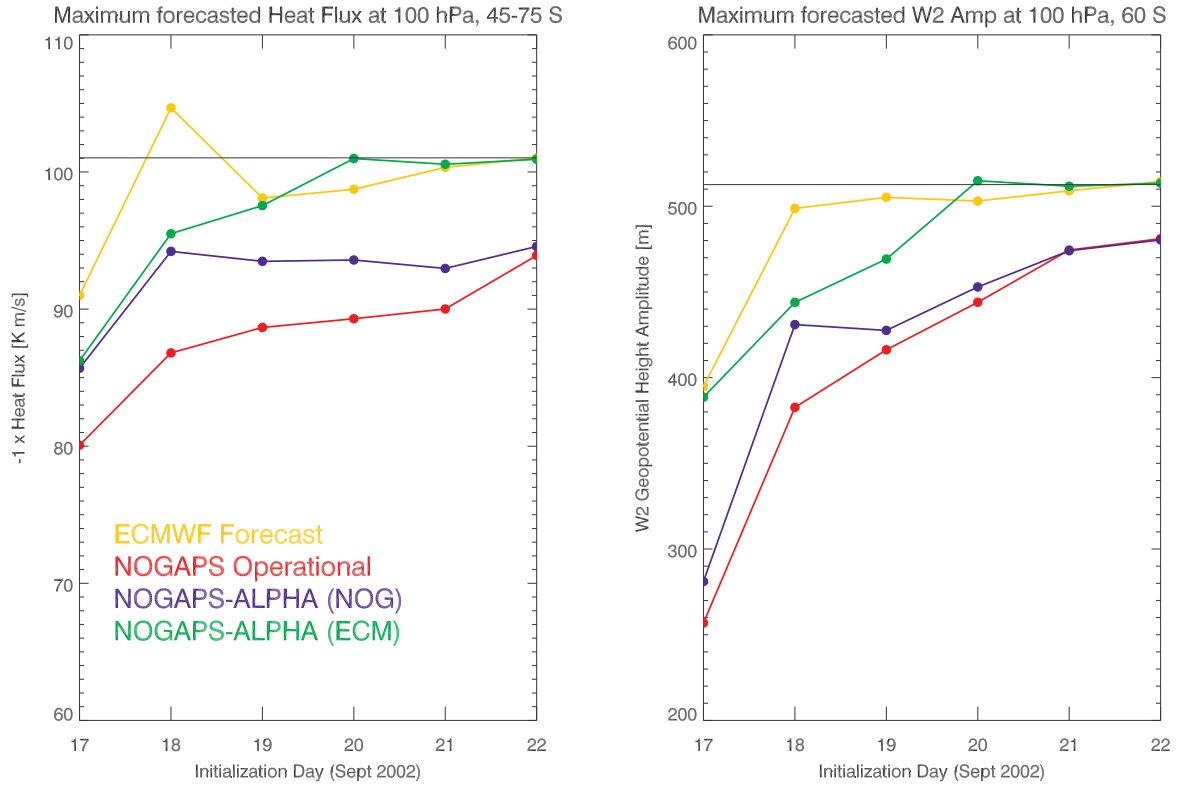


FIG. 10. (left) the maximum forecasted 100 hPa eddy heat flux (averaged from 45-75 S and multiplied by -1 to make poleward flux positive) and (right) the maximum zonal wave 2 amplitude at 100 hPa, 60 S for runs initialized from 17-22 September 2002.